YTUP

Journal of Thermal Engineering

https://jten.yildiz.edu.tr/

https://doi.org/10.47481/jten.0072

RESEARCH ARTICLE

# Exploring consequence of chemical reaction on MHD nanofluid flow above a nonlinearly extending sheet: applications in industrial coating processes

K.S. Behera[1], S.K. Parida[2,*], M.R. Acharya[3]

[1]Department of Mathematics., Faculty of Engineering and Technology, Siksha O Anusandhan University, Bhubaneswar - 751030, India
[2]Department of Mathematics., Faculty of Engineering and Technology, Siksha O Anusandhan University, Bhubaneswar - 751030, India
[3]Dept. of Physics, College of Basic Sc. & Humanities, OUAT, Bhubaneswar - 751003, India

## Abstract

The impact of a chemical process on nanofluid flow above a nonlinearly extending surface has been examined. The study also investigates mass and heat transfer, which have potential applications in industrial coating processes. Commonly, no-slip conditions are applied at the boundary of the flow regime. Instead, we include the velocity- and thermal-slip effects as an added aspect of the investigation when the nanofluid flows through a porous medium. The model is constructed using ordinary differential equations and after converted into partial differential equations via similarity transformations. A MATLAB program using the Keller-box method is employed to solve the modified equations. A Novel aspect of the combined effect of the magnetic field is the permeability parameter, and the chemical reaction was accounted for in the simulation of nanofluid flow over a nonlinear stretching surface. The study exhibits how different parameters affect the flow dynamics and flow features of nanofluid. It is seen that with an increase in a chemical reaction parameter, the reaction goes ahead at a faster rate, causing the concentration of the new product to increase. The research explores the impact of pertinent parameters on the dimensionless profiles of flow velocity, temperature, and mass concentration. Graphical representations are used to visualize the effects of key physical quantities in this study. The findings obtained are confirmed against previously published results.

**Keywords:** Nanoparticles, porous medium, keller-box method, non-linear stretching sheet

**Cite this article as:** Behera, K. S., Parida, S. K., & Acharya, M. R. (2026). Exploring consequence of chemical reaction on MHD nanofluid flow above a nonlinearly extending sheet: applications in industrial coating processes. Journal of Thermal Engineering, 12(5), 1873–1885. https://doi.org/10.47481/jten.0072

## 1. Introduction

The study of the nonlinear extending sheet is an important aspect of boundary layer theory which has practical applications in industry and engineering. Nanofluids have been found to show superior thermal performance compared to standard fluids, making them ideal for use in heat-transfer applications. The improved transfer ability of nanofluids can be attributed to the nanoparticles' high surface-area-to-volume ratio. This leads to enhanced interaction with the base fluid and more effective heat transfer. Furthermore, nanofluids show enhanced thermal behavior due to convection. Increases in thermal stability and specific heat capacity are also important in many applications. Nanofluids have these characteristics, making them suitable for various applications, including cooling electronic devices, managing heat transfer in heat exchangers, and augmenting the efficiency of solar collectors. By employing the homotropy analysis approach, Rashidi et al. [1] examined the time-independent flow in two dimensions of magneto hydrodynamics (MHD) in a porous medium. Using the Runge-Kutta method, Hady et al. [2] found viscous micro fluid heat radiation along a nonlinear expanding surface. An extensive array of applications is found in the polymer industry due to the flow of nanofluids over a linearly extending or contracting sheet. In this connection, Aman et al. [3] analyzed the flow above a linearly contracting sheet subjected to a magnetic field. Uddin et al. [4] experimented with Newtonian Nano fluid on enlarging sheet in two-dimension magneto hydrodynamics laminar free convicting flow over a boundary. Makinde and Aziz [5] carried out numerical research on flow beneath the

*Corresponding Author
E-mail Adress: sampadaparida@soa.ac.in

**Submitted:** 25 June 2025; **Accepted:** 18 October 2025

This paper was recommended for publication in revised form by Editor-in-Chief Ahmet Selim Dalkılıç

boundary of linear shrinking surface of a Nano fluid. R-K numerical procedure was used by Hamad et.al [6] to solve viscous flow of Nano fluid using similarity transformation. The Keller Box Method was used by Ramya et al. [7] to analyses velocity and slip condition on magneto hydrodynamic flow above a non-linear contracting sheet and the results were shown in tabular and graphical form. Ghazi et al. [8] described the size of a cold cylinder that affects the fluid flow and heat transfer in a triangular cavity with triangular shape filled with hybrid nanofluid, helping to improve cooling for solar panels. Goud et al. [9] examined unsteady magneto hydrodynamics flow on porous material under the influence of viscous dissipations for a non-scattering grey fluid and they noticed that Nano fluid temperature is inversely proportional to parameter of radiation. Jafer et al. [10] considered a non-linear expanding surface to find the phenomenon of heat radiation in the nanofluid flow in porous medium without Brownian diffusion and thermophoresis. In their research, the primary findings include an increase in fluid temperature due to Eckert numbers, the heat generation parameter, and the radiation parameter. Ahmad et al. [11] found the significance of heat control systems, engineering in biomedical, food factories by using multi slip magneto hydrodynamics nano fluid flow under bio convection effect. Abbas et al. [12] discuss fluid flow with homogeneous and heterogeneous reactions. Reddy and Reddy [13] examined magneto hydrodynamics flow above a horizontal shape of parabola with the impact of thermal radiations. Janke et al. [14] proved an analysis of nanofluid flow, considering the presence of dust particles that show a non-uniform heat effect, affecting both heat and momentum transfer. Khan et al. [15] discussed numerical survey of absorption of heat transfer and joule heating dissipation in a Nano fluid. Makkar and Batra [16] numerically investigated nanofluid flow in the presence of buoyancy forces in three-dimensional exponential shrinking sheet. Geetha [17] demonstrated the effects of suction and Stefan blowing of non-Newtonian nanofluid flows over an unstable stretched surface. Parida et al. [18] discussed mass transfer and heat convection past a flat heated plate considering thermophoresis particle deposition and slip conditions. The study proves that fluid characteristics are variable and that radiation is nonlinear. Hybrid ferro fluid flow above exponential stretching surface moving towards a stagnation point region analyzed by Anuar et al. [19]. Sadighi et.al. [20] explored the magneto hydrodynamics Nano fluid flow above a porous extending sheet with some inclination. An exact solution to the problem was also found in terms of the confluent hypergeometric function. Magneto hydrodynamic Sisko nano fluid flow with chemical reaction past a non-linearly stretching sheet was analyzed by Prasannakumara et.al. [21]. Transient nano fluid flow squeezing process involving aluminum oxide nano particles was investigated by Tlili et. al [22]. Application of neural network on heat transfer enhancement of magneto hydrodynamics nano fluid based on a new type of NN known as the group method of data handling (GMDH) was studied by Gerdroodbary et. al. [23]. Manh et. al. [24] reported influence of variable magnetic field on the flow pattern of nanofluid flow on a backward facing step. Again, Manh et. al. [25] solved magneto hydrodynamics nano fluid flow in non- parallel plates. Sedki [26] analyzed combined effect of thermal radiation and chemical reaction of mixed convection magneto hydrodynamics nano fluid flow passing over a non-linearly stretching sheet unsteady nature of magnetized nano fluid flow over a permeable stretching sheet was examined by Humance et. al. Ferro fluid flow in a screw tube with thermal performance was analyzed by Gerdrodbary et. al. [28]. Reddy et. al. [29] numerically investigated significance of radiation and chemical reaction for a magneto hydrodynamics nano fluid over a permeable linearly extending surface. Magneto hydrodynamic Jeffrey's nano fluid with velocity slip and thermal jump was investigated by Karishna et. al. [30] numerical investigation of flow dynamics of non-Newtonian tangent hyperbolic nano fluid above a non-linearly stretching sheet was carried out by Abbas et. al. [31]. The nanofluid flow and heat transfer over a nonlinearly stretching sheet with a variable magnetic field in a permeable medium have yielded significant applications in current fluid dynamics research owing to their many uses. However, no investigation has addressed the synergistic effect of variable magnetohydrodynamic, chemically reacting nanofluid flow over a nonlinearly stretched sheet in a porous medium. Therefore, the aim of this paper is to expand upon the findings of Ramya [7]. Nanofluid concentration is evaluated based on the motion of small particles in the fluid. The investigation also neglected the effects of suction or blowing. The research aims to investigate wall-slip flow and heat transfer of the nanofluid. The finite-difference-based Keller-box method has been applied to obtain numerical solutions to the problem. The main finding obtained here is physically interpreted in this paper.

## 2. Mathematical model

Electrical conducting two-dimensional flow of viscous laminar steady incompressible Nano fluid across a surface undergoing non-linear expansion with a velocity  from a fixed origin is considered in this study. The flow occurs only in the upper parts of the plate .  Surface stretching begins at the origin. The stretching force induces flow along the x-axis see Figure 1). The sheet temperature and the nanoparticle fractions of the stretched sheet are treated as constants. Similarly, ambient temperature and nanoparticle fraction are treated as constants. The momentum equation accounts for the effects of a permeable medium and the slip conditions at the wall. Chemical reaction effects contribute to mass transfer phenomena.

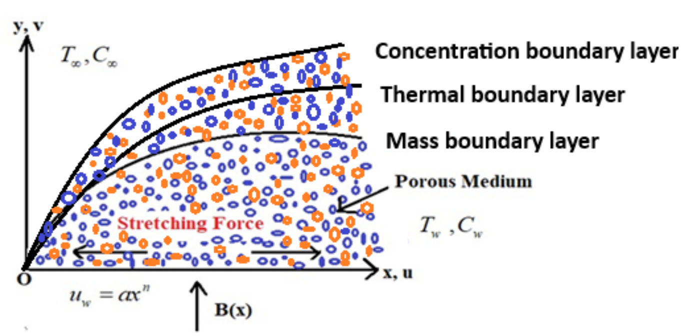


**Figure 1.** Flow configuration

The transport model of nano fluid is based on the following assumptions.

i. The fluid is incompressible. (constant)
ii. External forces are treated negligible.
iii. The volume fraction is less than one.
iv. Base fluid and nano fluid are locally in thermal equilibrium.

The equations (1)-(4) being the mathematical formulation of Nano fluid problem are

$$u_x = -v_y \tag{1}$$

$$uu_x + vu_y - \nu u_{yy} = -\left(\frac{\nu u}{K_p^*} + \frac{\sigma B^2(x)}{\rho_f}u\right) \tag{2}$$

$$-\alpha T_{yy} + uT_x + vT_y = \frac{\nu}{c_p}(u_y)^2 + \tau\left(\frac{D_T}{T_\infty}(T_y)^2 + D_B T_y C_y\right) \tag{3}$$

$$-\frac{D_T}{T_\infty}(T_{yy}) + uC_x - K_1^*(C - C_\infty) = D_B C_{yy} - vC_y \tag{4}$$

Where $\alpha =, \frac{K}{(\rho c)_f}$ and $\tau = \frac{(\rho c)_p}{(\rho c)_f}$.

The fluctuating magnetic strength is $B(x) = B_0 x^{\frac{n-1}{2}}$.

The flow conditions at the boundary are specified by

$$\left.\begin{array}{ll} v = 0, u = u_w + Nu_y, C = C_w, T = DT_y + T_w & \text{when } y = 0 \\ v \to 0, u \to 0, C = C_\infty, T = T_\infty & \text{when } y \to \infty \end{array}\right\} \tag{5}$$

Here $u_w = ax^n$ is the nonlinear velocity associated with stretching and sheet temperature $T_w = T_\infty + bx^{2n}$, where a and b are constants $N = N_1 x^{\frac{1-n}{2}}$, is the variable velocity slip, $D = D_1 x^{\frac{1-n}{2}}$ and $N_1$ is the starting velocity slip. is the variable thermal slip, $D_1$ is the first thermal slip and N=D=0 means no-slip.

The transformation leading to non-dimensional aspect are defined as

$$\left.\begin{array}{l} u = af'(\eta)x^n,\ \eta = \sqrt{\frac{a(n+1)}{2\nu_f}}x^{\frac{n-1}{2}}y \\ v = -\sqrt{\frac{a\nu_f}{2(n+1)}}((n+1)f(\eta) + (n-1)\eta f'(\eta))x^{\frac{n-1}{2}} \\ T = b\theta(\eta)x^{2n} + T_\infty,\ \phi(\eta) = \frac{(C - C_\infty)}{(C_w - C_\infty)} \end{array}\right\} \tag{6}$$

Using equations (5), (6) and (11), equations (2-4) reduce to

$$f''' - \left(\frac{2n}{n+1}\right)f'^2 = (M + K_p)f' - ff'' \tag{7}$$

$$\theta'' + Pr\left((Nt)\theta'^2 + \theta'(f + (Nb)\phi') + (Ec)f''^2 - \left(\frac{4n}{n+1}\right)\theta f'\right) = 0 \tag{8}$$

$$\phi'' + (Le)f\phi' - K1\phi + \frac{Nt}{Nb}\theta'' = 0 \tag{9}$$

The associated conditions (5), then become

$$\left.\begin{array}{ll} f' = \lambda f''(0) + 1, f = 0, \theta = \delta\theta'(0) + 1, \phi = 1 & \text{when } \eta = 0 \\ \theta \to 0, \phi \to 0, f' \to 0 & \text{when } \eta \to \infty \end{array}\right\} \tag{10}$$

The parameters evolved are described below.

$$\left.\begin{array}{l} Le = \frac{\nu_f}{D_B},\ M = \frac{2\sigma B_0^2}{a\rho_f(n+1)}, \\ Nb = \frac{D_B(\rho c)_p(C_w - C_\infty)}{(\rho c)_f \nu_f}, \\ Nt = \frac{D_T(\rho c)_p(T_w - T_\infty)}{(\rho c)_f \nu_f T_\infty}, \\ \lambda = N_1\sqrt{\frac{a(n+1)\nu_f}{2}},\ \delta = D_1\sqrt{\frac{a(n+1)}{2\nu_f}}, \\ Ec = \frac{u_w^2}{c_p(T_w - T_\infty)},\ K_p = \frac{2\nu}{aK_p^*(n+1)}x^{1-n}, \\ K1 = \frac{2K_1^*\nu_f}{aD_B(n+1)x^{n-1}},\ Pr = \frac{\nu_f}{\alpha} \end{array}\right\} \tag{11}$$

The quantities of importance equations (12)-(14) in this analysis are specified as

$$\begin{array}{ll} C_{fx} = \frac{\mu_f}{\rho u_w^2}\frac{\partial u}{\partial y}\Big|_{y=0} & \text{(Skin friction)} \\ Nu_x = \frac{q_w x}{k(T_w - T_\infty)} & \text{(Nusselt number)} \\ Sh_x = \frac{q_m x}{D_B(C_w - C_\infty)} & \text{(Sherwood number)} \end{array} \tag{12}$$

where

$$q_w = -k\frac{\partial T}{\partial y}\Big|_{y=0},\ q_m = -D_B\frac{\partial C}{\partial y}\Big|_{y=0} \tag{13}$$

$$\left.\begin{array}{l} Re_x^{\frac{1}{2}}C_{fx} = \left(\frac{n+1}{2}\right)^{\frac{1}{2}}f''(0),\ Re_x^{-\frac{1}{2}}Nu_x = -\left(\frac{n+1}{2}\right)^{\frac{1}{2}}\theta'(0), \\ Re_x^{-\frac{1}{2}}Sh_x = -\left(\frac{n+1}{2}\right)^{\frac{1}{2}}\phi'(0) \end{array}\right| \tag{14}$$

Where $Re_x = \frac{u_w x}{\nu}$ (Local Reynolds number).

## 3. Method

The closed-form solutions to equations (7)-(9) are infeasible due to the nonlinear nature of the equations. Therefore, the results are obtained numerically by employing Keller-box scheme subject to boundary conditions (10). A few key steps related to the scheme are described below (Figure 2). Although the Keller box method requires slightly more arithmetic compared with other methods, it has the following advantages.

1. Its accuracy is second order finite difference method with arbitrary spacing in x and y.
2. x can vary very rapidly
3. Many coupled equations can be solved by this method because it yields a block-tridiagonal system that is stable, correct, and easy to solve.

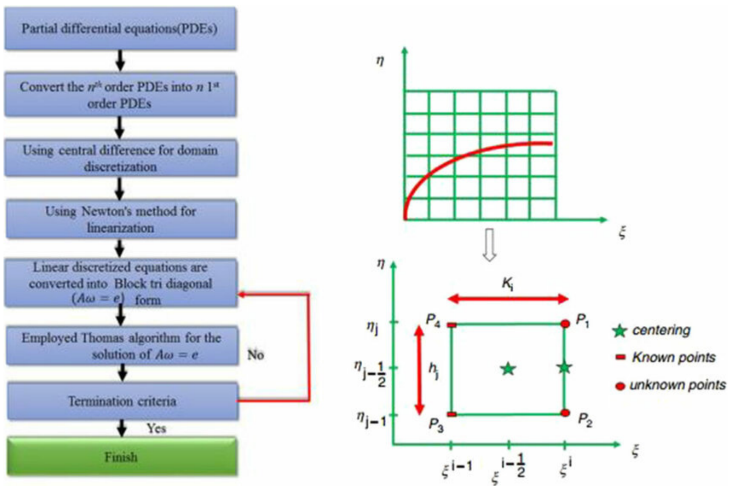


**Figure 2.** Keller Box Scheme

Transforming higher order nonlinear ODEs into linear 1st order differential equations through assumptions.

$$f' = p, p' = q, \theta' = t, \phi' = v \tag{15}$$

Using (15), the central difference method converts 1st order differential equations into discrete difference equations.

$$p_j - \frac{h_j}{2}q_j = -\frac{h_j}{2}q_{j-1} + p_{j-1} \tag{16}$$

$$f_j - \frac{h_j}{2}p_j = -\frac{h_j}{2}p_{j-1} + f_{j-1} \tag{17}$$

$$\theta_j - \frac{h_j}{2}t_j = -\frac{h_j}{2}t_{j-1} + \theta_{j-1} \tag{18}$$

$$\phi_j - \frac{h_j}{2}v_j = -\frac{h_j}{2}v_{j-1} + \phi_{j-1} \tag{19}$$

Nonlinear equations undergo linearization via Newton's methods, transforming them into a specific form using equations (16)-(19).

$$\delta f_j = \frac{h_j}{2}(\delta p_j - \delta p_{j-1}) + (r_1)_{j-\frac{1}{2}} + \delta f_{j-1} \tag{20}$$

$$\delta p_j = \frac{h_j}{2}(\delta q_j - \delta q_{j-1}) + (r_2)_{j-\frac{1}{2}} + \delta p_{j-1} \tag{21}$$

$$\delta\theta_j = \delta\theta_{j-1} + (r_3)_{j-\frac{1}{2}} + \frac{h_j}{2}(\delta t_j - \delta t_{j-1}) \tag{22}$$

$$\delta\phi_j = (\delta v_j - \delta v_{j-1})\frac{h_j}{2} + \delta\phi_{j-1} + (r_4)_{j-\frac{1}{2}} \tag{23}$$

$$\delta q_j(a_1)_j + \delta f_j(a_3)_j + +\delta p_j(a_5)_j = (r_5)_{j-\frac{1}{2}} - \delta q_{j-1}(a_2)_j - \delta f_{j-1}(a_4)_j - \delta p_{j-1}(a_6)_j$$
$$(b_1)_j\delta t_j + (b_3)_j\delta f_j + (b_5)_j\delta p_j + (b_7)_j\delta\theta_j + (b_9)_j\delta v_j + (b_{11})_j\delta q_j = (r_6)_{j-\frac{1}{2}} \tag{24}$$

$$-(b_2)_j\delta t_{j-1} - (b_4)_j\delta f_{j-1} - (b_6)_j\delta p_{j-1} - (b_8)_j\delta\theta_{j-1} - (b_{10})_j\delta v_{j-1} - (b_{12})_j\delta q_{j-1} \tag{25}$$

$$(c_1)_j\delta v_j + (c_3)_j\delta f_j + (c_5)_j\delta t_j = (r_7)_{j-\frac{1}{2}} - (c_2)_j\delta v_{j-1} - (c_4)_j\delta f_{j-1} - (c_6)_j\delta t_{j-1}$$
$$-(c_7)_j\delta\phi_{j-1} - (c_8)_j\delta\phi_{j-1} \tag{26}$$

where,

$$\left.\begin{aligned}&(a_1)_j - 1 = \frac{h_j}{2}f_{j-\frac{1}{2}}, (a_1)_j - (a_2)_j = 2, (a_4)_j = (a_3)_j = \frac{h_j}{2}q_{j-\frac{1}{2}},\\ &(a_5)_j = (a_6)_j = -\left(\frac{2n}{n+1}\right)h_j p_{j-\frac{1}{2}} - \frac{M}{2}h_j - \frac{K_p h_j}{2},\end{aligned}\right\} \tag{27}$$

$$\left.\begin{aligned}&(b_1)_j = \frac{1}{p_r} + \frac{h_j}{2}f_{j-\frac{1}{2}} + \frac{h_j Nb}{2}v_{j-\frac{1}{2}} + h_j Nt(t_{j-\frac{1}{2}}),\\ &(b_2)_j = -\frac{1}{p_r} + \frac{h_j}{2}f_{j-\frac{1}{2}} + \frac{h_j Nb}{2}v_{j-\frac{1}{2}} + h_j Nt(t_{j-\frac{1}{2}}), (b_3)_j = (b_4)_j = \frac{h_j}{2}t_{j-\frac{1}{2}},\\ &(b_5)_j = (b_6)_j = -\frac{h_j}{2}\left(\frac{4n}{n+1}\right)\theta_{j-\frac{1}{2}}, (b_7)_j = (b_8)_j = -\frac{h_j}{2}p_{j-\frac{1}{2}}\left(\frac{4n}{n+1}\right),\\ &(b_9)_j = (b_{10})_j = \frac{h_j}{2}Nbt_{j-\frac{1}{2}}, (b_{11})_j = (b_{12})_j = \frac{h_j Ec}{2}q_{j-\frac{1}{2}},\end{aligned}\right\} \tag{28}$$

$$\left.\begin{aligned}&(c_1)_j - 1 = \frac{h_j}{2}Le(f_{j-\frac{1}{2}}), (c_1)_j - (c_2)_j = 2, (c_3)_j = (c_4)_j = \frac{h_j}{2}Le(v_{j-\frac{1}{2}}),\\ &Nt = Nb(c_5)_j, (c_6)_j = -(c_5)_j, (c_8)_j = (c_7)_j = -h_j K1,\end{aligned}\right\} \tag{29}$$

$$\begin{aligned}&f_j = f_{j-1} + h_j(p_{j-\frac{1}{2}}) - (r_1)_j, p_j = p_{j-1} + h_j(q_{j-\frac{1}{2}}) - (r_2)_j, \theta_j\\ &\quad = \theta_{j-1} + h_j(t_{j-\frac{1}{2}}) - (r_3)_j,\\ &\phi_j = \phi_{j-1} + h_j(v_{j-\frac{1}{2}}) - (r_4)_j, q_j = q_{j-1} + h_j\left(\frac{2n}{n+1}\right)p^2_{j-\frac{1}{2}}\\ &+Mh_j p_{j-\frac{1}{2}} + K_p h_j p_{j-\frac{1}{2}} - h_j(fq)_{j-\frac{1}{2}} - (r_5)_j,\\ &\frac{1}{p_r}(t_j) + (r_6)_j = \frac{1}{p_r}t_{j-1} + h_j\left(\left(\frac{4n}{n+1}\right)p_{j-\frac{1}{2}}\theta_{j-\frac{1}{2}} - f_{j-\frac{1}{2}}t_{j-\frac{1}{2}} - Nbt_{j-\frac{1}{2}}v_{j-\frac{1}{2}}\right)\\ &-Ech_j q^2_{j-\frac{1}{2}} - Nth_j t^2_{j-\frac{1}{2}}\\ &v_j + (r_7)_j - K1h_j\phi_j = -h_j(K1\phi_{j-1} + Lef_{j-\frac{1}{2}}v_{j-\frac{1}{2}}) + v_{j-1}\\ &-\left(\frac{Nt}{Nb}\right)(t_j - t_{j-1})\end{aligned} \tag{30}$$

Using MATLAB, block elimination technique solves linear equation system equations (20)-(26) for the values of equations (27)-(30) through systematic elimination processes.

## 4. Validation of problem formulation

As said above, we use the Keller–Box scheme to obtain the solution of the nonlinear ordinary differential equations (7)– (9) and (10). The step size is pertinent to this investigation. The error tolerance is sufficient to conduct numerical simulation. The parameter values used for calculations are Pr = 6.8, Ec = 0.1, n=1, λ = 0.1, Le = 5, M = 1, Nt = 0.3, Nb = 0.3, δ = 0.1, Kp = 0.5, K1 = 0.1.To evaluate the reliability and precision of the employed numerical approach, the values of Pr ,Ec ,n, λ, Le, M, Nt, Nb, δ , Kp , K1 are chosen to analyses our findings with that of Ramya et al. [7] . The physical quantities for this flow analysis are the $C_f Nu_x$ and $Sh_x$, and are calculated and depicted through graphs. To confirm confirmed mathematical formulation, the skin friction results (Table-1) obtained from Hamad et.al [6] and Ramya et.al [7] relates to the present results. The present results confirm our formulation and application of numerical simulation against existing literature.

**Table 1.** Skin friction constants for different values of Le = 1, Ec = 0.1, Pr = 6.8, $K_p$ = M = λ = δ = Nb = $K_1$ =Nt = 0

| N | Present study | Hamad et al. [6] | Ramya et al. [7] |
|---|---|---|---|
| 0 | 0.6285 | 0.6283 | 0.6283 |
| 0.2 | 0.7677 | 0.7674 | 0.7675 |
| 0.5 | 0.8905 | 0.8901 | 0.8901 |
| 1.0 | 1.0005 | 1.0004 | 1.0005 |
| 3.0 | 1.1494 | 1.1489 | 1.1490 |
| 10 | 1.2356 | 1.2352 | 1.2352 |
| 20 | 1.2579 | 1.2577 | 1.2578 |

## 5. Result

Figure 3 to Figure 5 provide insights into the presence of magnetic parameter (M) on the flow, thermal, and concentration distribution of the nanofluid. Specifically, Figure 3 illustrates how M influences the movement of the nanofluid. It is found that nanofluid's velocity decreases for large values of M. This decrease can be attributed to the Lorentz force experienced by charged nanoparticles moving through a magnetic field, effectively acting as a drag force. Figure. 4 illustrates how the temperature distribution is influenced by parameter M. As the magnetic field values increase, the thermal field also rises. These phenomena can be clarified by considering the impact of the Lorentz force from the transverse magnetic field, which has a significant effect on the relaxation of fluid temperature and velocity distributions.

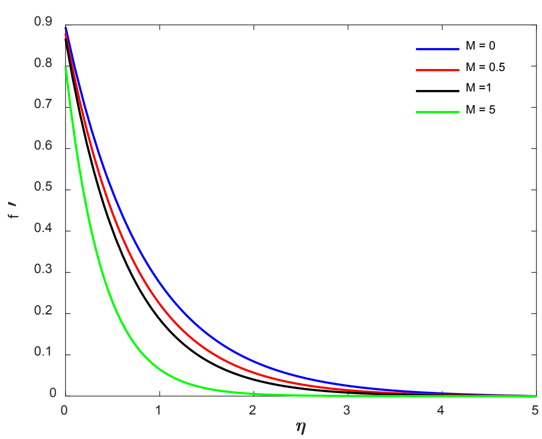


**Figure 3.** Velocity distribution for M

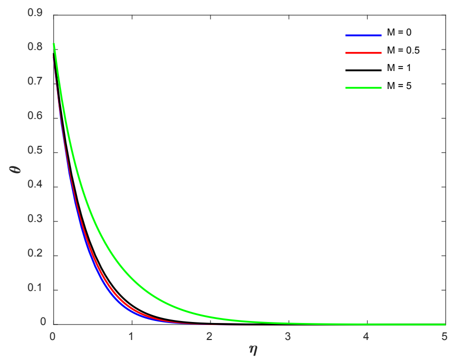


**Figure 4.** Temperature variation for M

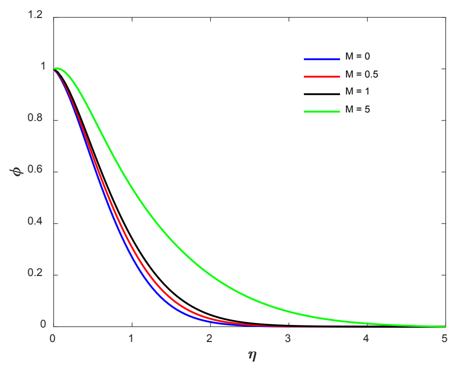


**Figure 5.** Concentration distribution for different M

Figure 5 shows the concentration profile. The data clearly show a continuous rise in concentration as the values of M increase. This effect is caused by the progressive increase in the thickness of the concentration profiles due to the application of a magnetic field. Overall, the Figure shows how M plays a vital role in shaping the flow velocity, thermal distribution, and mass distribution of the nanofluid.

Figures 6-8 present the impact of [velocity slip parameter] on the flow of velocity profiles. In Figure 6, increments allow a reduction in the velocity profile of the nanofluid owing to stronger coupling and increased drag force.

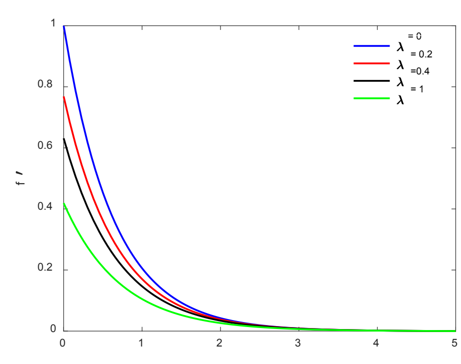


**Figure 6.** Dependence of velocity on λ

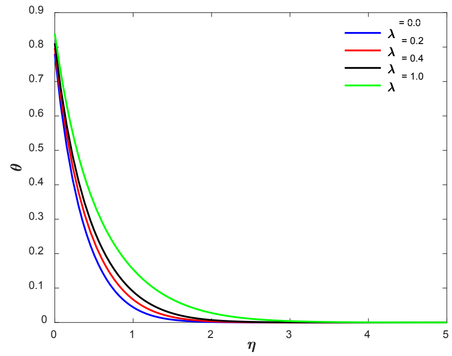


**Figure 7.** Variation of temperature on

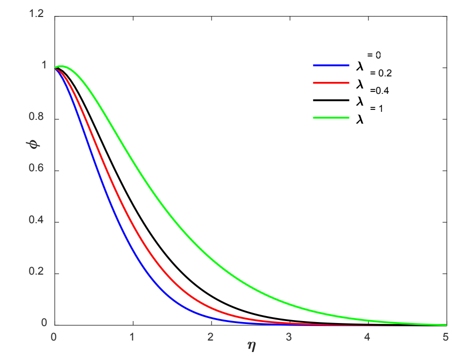


**Figure 8.** Concentration dependence on λ

However, contrasting results are seen in Figures 7 and 8 for the thermal and mass distributions of the nanofluid. In these Figure, this leads to an opposite effect, causing an increase in both temperature and concentration distributions. The impact of the thermal slip parameter on the temperature and concentration distributions is shown in Figures 9 and 10, respectively. Figure 9 shows that as the parameter increases, the temperature of the nanofluid decreases. Interestingly, even a small amount of heat supplied to the fluid reduces the thermal boundary layer thickness as the parameter values increase. In Figure 10, it is shown that it shows a noticeable decrease as the parameter increases.

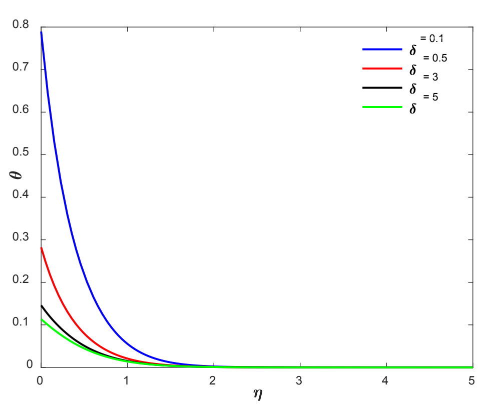


**Figure 9.** Dependence of temperature on δ

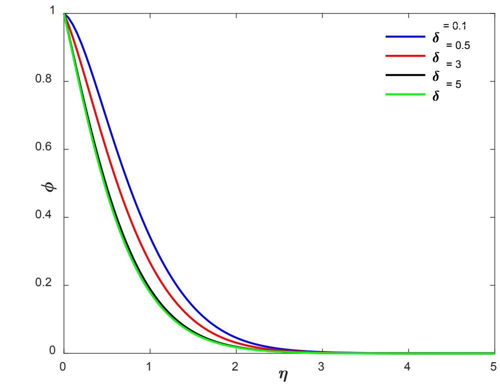


**Figure 10.** Concentration variation for

The role of on all profiles is shown in Figures 11-13. The significance of permeable parameters ($K_p$) on the flow velocity profile is conveyed in Figure 11. An increment in implies a more concentration of solid nanoparticles dispersed in the base fluid, leading to elevated viscosity and decreased Nano fluid velocity. Figures 12 and 13 display the impact of on both temperature and concentrations profiles. Temperature and concentration are also increased when rises because it increases the medium's porosity and strengthens the viscous forces.

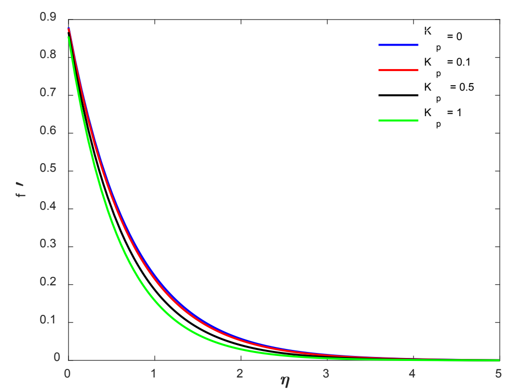


**Figure 11.** Dependence of velocity on δ

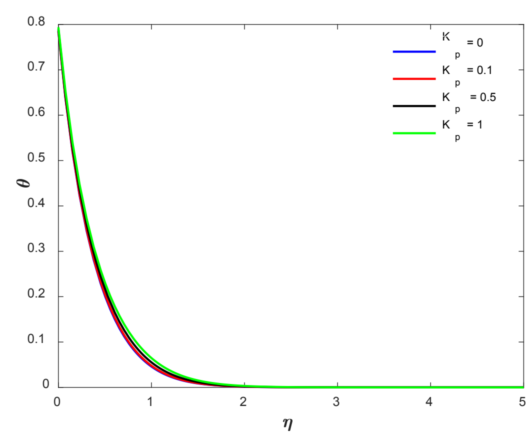


**Figure 12.** Dependence of temperature for $K_p$

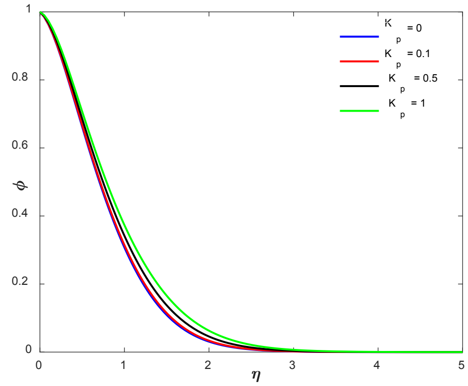


**Figure 13.** Variation of concentration for $K_p$

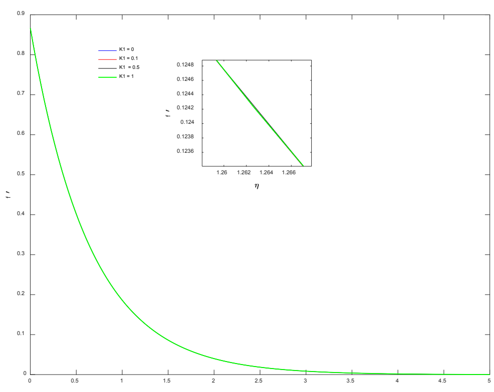


**Figure 14.** Dependence of velocity on K1

The influence of [chemical reaction parameter] on all profiles is shown in Figures 14–16. Enhancement of chemical reaction parameters imply a decrease in fluid velocity (Figure 14). This illustrates that the rate of any chemical reaction depends on temperature, pressure, concentration, surface area, etc. Figure 15 reveals that the thermal boundary layer of the nanofluid decreases with an increase in the chemical reaction parameter. Physically, a higher chemical reaction rate implies faster molecular motion and thus reduces the temperature.

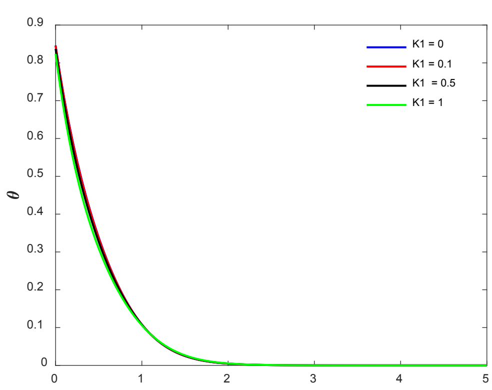


**Figure 15.** Variation of temperature for K1

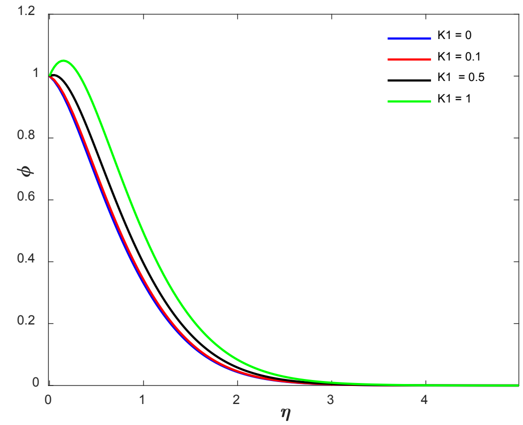


**Figure 16.** Variation of concentration for K1

Figure 16 illustrates the effect of the chemical reaction parameter on the mass distribution profile for several values of the parameter. The dimensionless concentration equals unity at the wall and approaches zero far from the sheet. When $C_w > C_\infty$ there is a rapid drop off concentration for lower values of as portrayed in the curve. When stronger, the concentration of nanofluid near the wall exceeds the wall concentration and then drops to zero far from the sheet. The chemical reaction goes ahead in the forward direction, showing the formation of a product. The faster the chemical reaction, the larger the thickness of the boundary layer.

The role of the factor in the thermal and mass distribution profiles is discussed in Figures 17 and 18. Figure 17 shows that an increase in value corresponds to a gradual increase in temperature. This phenomenon occurs due to a decrease in the rate of heat transfer near the surface of the stretched sheet. Figure 18 shows that, as the concentration values increase, they first decrease and then increase.

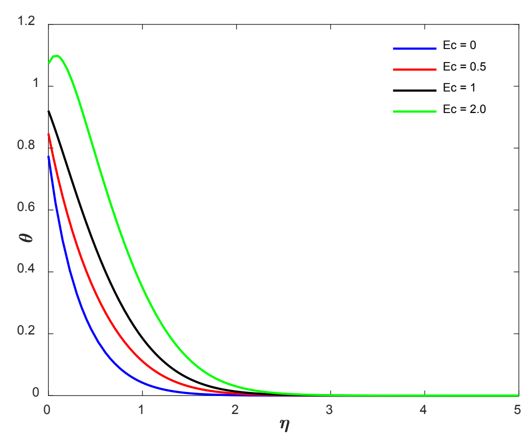


**Figure 17.** Temperature dependence on Ec

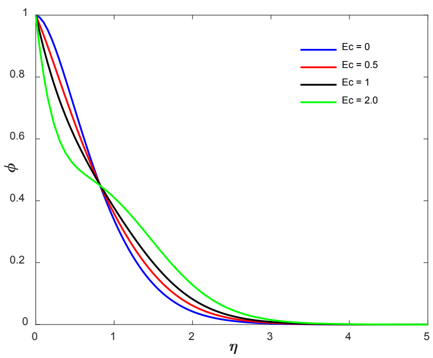


**Figure 18.** Concentration dependence on Ec

Figure 19 and Figure 20 display the impact on  the temperature and mass distribution profiles. An increased  denotes (Figure 19) a greater thermophoretic impact resulting from nanoparticles in the nanofluid shifting toward higher temperatures. This causes a build-up of the nanoparticles in the vicinity of the heated non-linear expanding surface, resulting in an increase in the nanofluid temperature. However, Figure 20 shows that the nanoparticle concentration in the nanofluid increases as nanoparticles migrate towards regions with higher temperatures. Because of thermophoretic forces, nanoparticles tend to concentrate in regions of higher temperature. At higher values, the concentration sharply rises above the wall value and then rapidly drops to zero in the ambient environment.

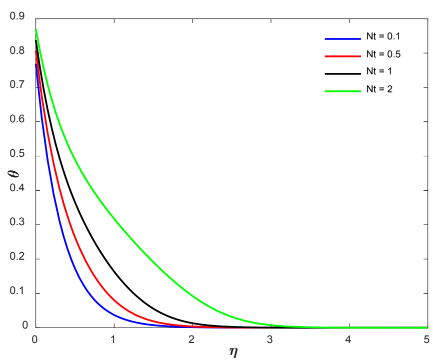


**Figure 19.** Temperature profile for change of Nt

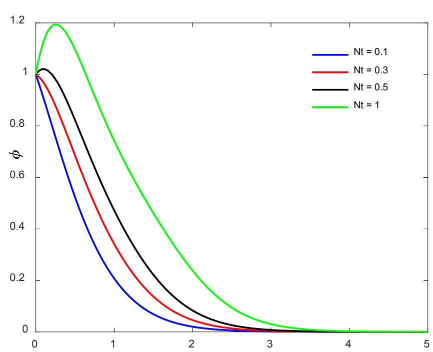


**Figure 20.** Dependence of concentration on Nt

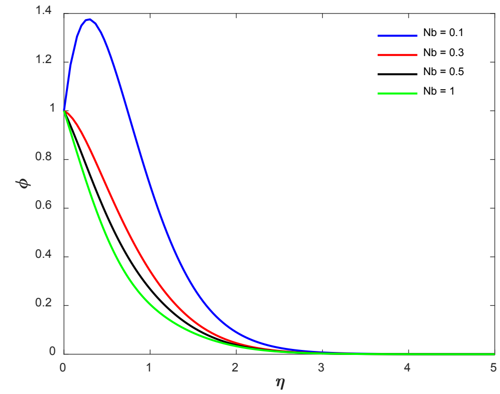


**Figure 21.** Dependence of concentration on Nb

Figures 21 and 22 display the impact of  [Brownian parameter] on both temperature and concentration profiles.  The effect of nanofluid temperature is shown in Figure 21. When  is increased, the temperature of the nanofluid increases. This is since rise in diffusion parameter refers to an increase in Brownian motion, which improves particles dispersion and combining in the fluid, however changing the value of Nb does not result in any noticeable changes on the concentration distribution as seen in Figure 22,

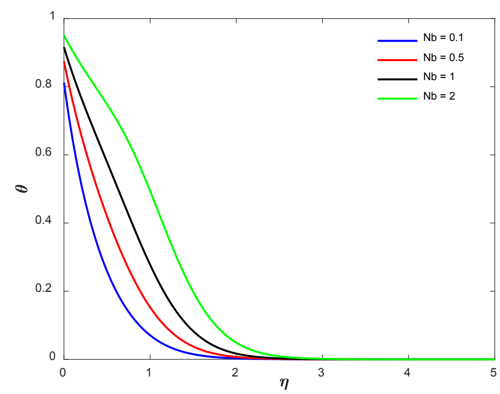


**Figure 22.** Dependence of temperature on Nb

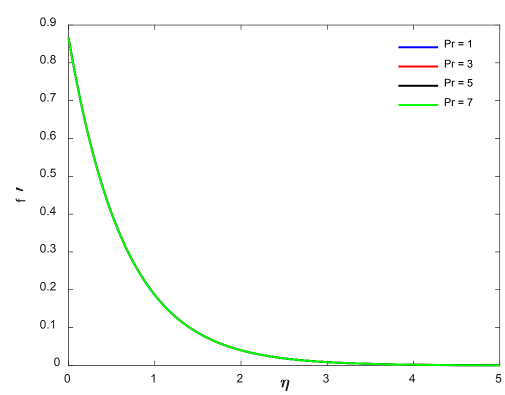


**Figure 23.** Distribution of velocity with respect to Pr

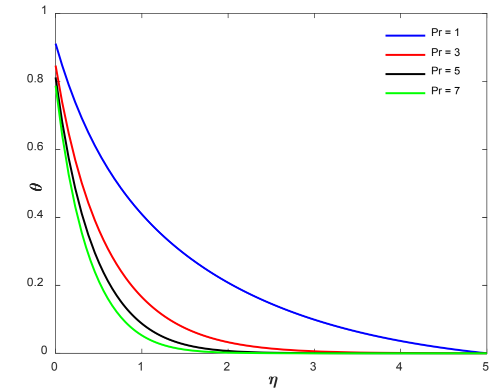


**Figure 24.** Dependence of temperature on Pr

The impact on all profiles is shown in Figures 23 through 25. In Figure 23, an increase is followed by a decrease in velocity. The role of temperature distribution is depicted in Figure 24. The increase in Pr in this Figure indicates that convective heat transfer induced by fluid flow now predominates overheat conduction. Consequently, convective heat transfer exceeds conduction, and the temperature of the nanofluid decreases. In Figure 25, an increase in Pr causes the concentration to rise.

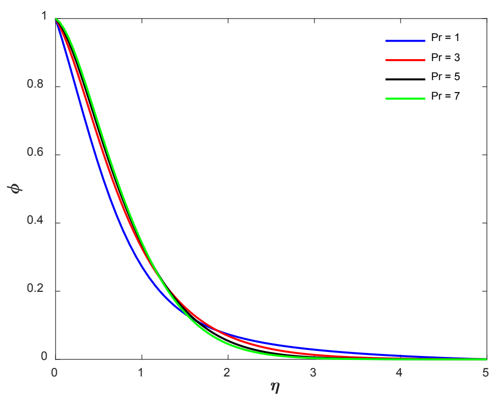


**Figure 25**. Variation of concentration for Pr

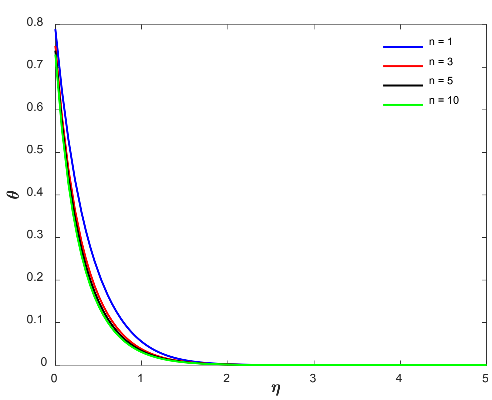


**Figure 26.** Dependence of temperature on n

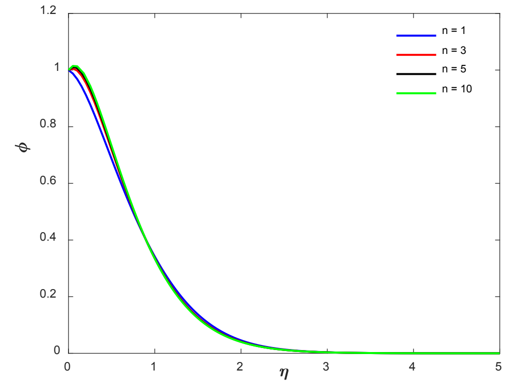


**Figure 27.** Concentration dependence on n

The role of  on thermal and concentration profile is drawn in Figure 26 and Figure 27. The temperature drops in Figure 26 as the values of rises, while the concentration profile in Figure 27 shows the opposite trend. Figure. 28 and Figure 29 prove how  affects the temperature and concentration distribution. In Figure 28, as  increases, the temperature rises, while the concentration profile shows the opposite effect, as depicted in Figure 29.

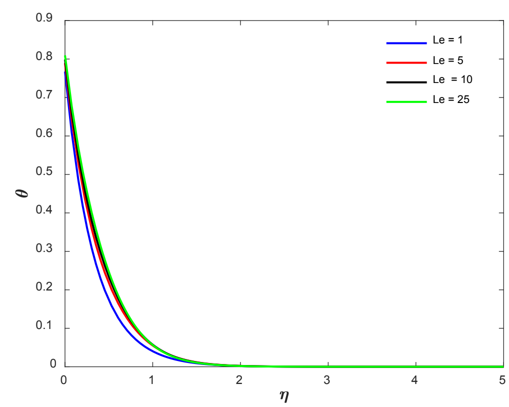


**Figure 28.** Temperature dependence on Le

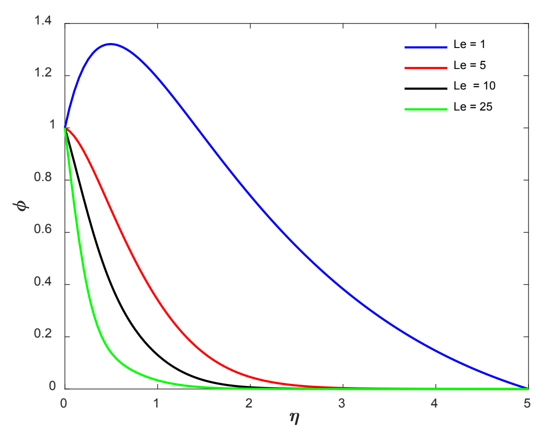


**Figure 29.** Concentration on variation of Le

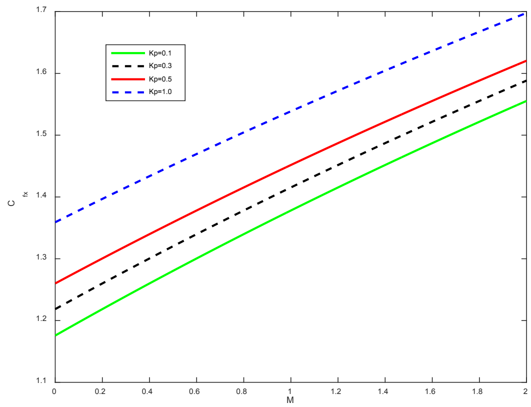


**Figure 30.** Skin friction $C_{fx}$ verses M for Kp

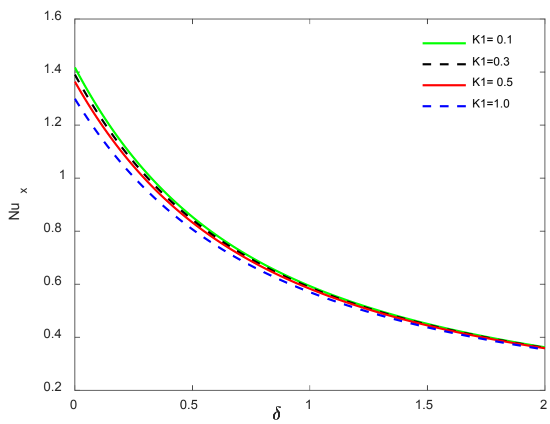


**Figure 31.** Heat transfer ratio $Nu_x$ verses δ for different values of K1

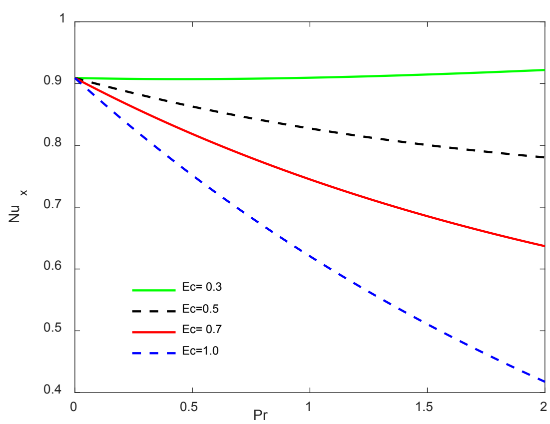


**Figure 32.** Variation of $Nu_x$ for Ec against Pr

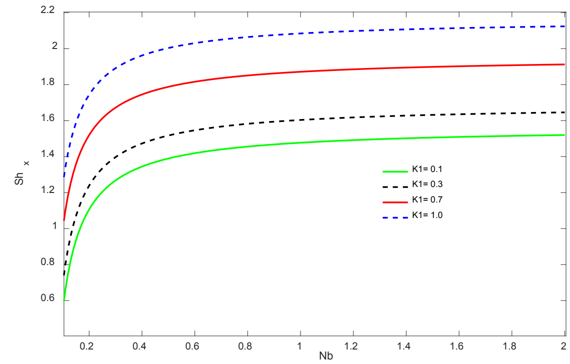


**Figure 33.** Dependence of $Sh_x$ on K1 against Nb

The influence of $K_p$ on skin friction against is shown in Figure.30. Increasing the value of $K_p$ enhances the skin-friction coefficients. This is credited to the intensified relationship among the magnetic field and the fluid due to the enhanced $K_p$, so increasing the width of the boundary layer. Ultimately, this results in an increased skin-friction coefficients with respect to the magnetic parameters. The impact of on Nusselt number against the thermal slip parameter is depicted in Figure.31. As is increased, the Nusselt number decreases.

The impact of on Nusselt number against is plotted in Figure.32. When we increase the value of then the coefficients of heat transfer diminish due to a higher values (> 5). Thus, fluid motion is favored due to thermal diffusions for heat transfer. Moreover, a high value shows that fluid motion due to conduction is preferred than heat transmission. When the Eckert number refers to the work done against viscous-fluid-forces. Kinetic energy is transformed into internal energy. Consequently, raising leading to enhancement in temperature distribution of the fluid. The influence of on Sherwood number against is depicted in Figure 33. The value of the Brownian motion enhances the Sherwood number as increases.

## 6. Discussion

The present study is entirely theoretical and depends on numerical simulations, with no experimental work. The prescribed boundary conditions, such as slip-wall temperature and sheet velocity, accurately reflect the dynamic nature of industrial coating processes, in which fluctuations in sheet motion and heating are common. Additionally, in actual industrial environments, electromagnetic fields can vary both spatially and temporally, potentially altering the flow behavior in ways not captured by the model. The adoption of a single-phase nanofluid model further simplifies the problem, potentially overlooking key microscale phenomena such as nanoparticle slip and thermophoresis. These interactions can significantly influence heat and mass transfer but are not adequately addressed in the current framework. The combination of nanoparticles and base fluid may not interact favorably with the substrate, potentially leading to issues such as poor adhesion, clogging, or surface degradation. Achieving consistent coating thickness and uniformity is particularly challenging to model in a dynamic industrial setting. Moreover, the implementation of nanofluid-based magnetohydrodynamic coating systems requires high-precision equipment, which can be costly. The study does not account for the economic viability or energy demands associated with deploying such advanced technologies in real-world applications.

## 7. Conclusion

The impact of several physical quantities on the flow of nanofluid above a nonlinearly extending sheet has been analyzed, and physical interpretations have been drawn from the graphs. The results are summarized below.

- Velocity shows a declining trend with the enhancement in K1, M, $K_p$, λ,and Pr.
- The thermal behavior of the Nano fluid exhibit increasing trend for the values of M, Nt, Nb, Ec, Le, λ and opposite trend in respect of; $K_p$,Pr, δandn.
- Concentration profile shows rising trend with respect to M, K1, δ,$K_{p,}$, λ, Nt and $K_{p,}$ and reverse trend for higher values of Nb, Le.
- The concentration distribution falls rapidly from a maximum value to zero in the ambient medium at lower values of the chemical reaction parameter. However, the concentration exceeds the value at the wall near the sheet for higher values of the chemical reaction parameter and then falls to zero away from the surface.
- Permeability parameter $K_p$ , enhances skin friction.
- Heat transfer coefficient is inversely related to K1 and Ec.
- Increase in mass transfer due to Brownian diffusion.

## Author contributions statement

Kanheya Subhamaya Behera: conceptualization, formal analysis, writing – original draft, writing. Sampada Kumar Parida: conceptualization, method, software, review & editing, supervision. Manas Ranjan Acharya: formal analysis, writing, editing

## Declaration of interests

The authors declare no competing financial or personal interests related to this work.

## Data availability

The data supporting the findings of this study are available within the manuscript. No data used in this study is confidential.

## Declaration of generative AI and AI-assisted technologies in the writing process

The authors declare that no generative AI or AI-assisted technologies were used in the preparation, writing, editing, or revision of this manuscript.

## List of abbreviations

| | |
|---|---|
| (u, v) | Nano fluid velocities |
| $u_w$ | Wall velocity |
| B(x) | Varying magnetic field |
| $K^*_p$ (x) | Permeability |
| $T_w$ | Wall temperature |
| $(pc)_p$ | Specific heat |
| $c_{fx}$ | Skin-friction |
| $Sh_x$ | Sherwood number |
| n | Nonlinear Extending parameter |
| $N_1$ | Velocity slip factor |
| $D_{1:}$ | Thermal slip factor |
| α | Thermal diffusivity |
| ν | Kinematic viscosity |
| K1 | chemical reaction parameter |
| Ec | Eckert number |
| $K_p$ | Porosity parameter |
| f | Dimensionless stream function |
| Pr | Prandtl number |

## Subscripts

| | |
|---|---|
| f | Fluid |
| w | Wall |
| m | Surface thermal parameter |
| δ ,λ | Thermal and velocity slip parameter |
| ρ | Density of fluid |
| μ | Viscosity related to the fluid |
| $(pc)_p f$ | Fluid Specific heat |
| T | Fluid temperature |
| $Nu_x$ | Nusselt number |
| $T_\infty$ | Ambient particle temperature |
| σ | Electrical conductivity |
| $C_w$ | Nanoparticle concentration |
| $C_\infty$ | Ambient nanoparticle concentration |
| Nt: | Thermophoresis parameter |
| M | Magnetic parameter |
| ϕ | Dimensionless concentration |
| Le | Lewis number |
| Nb | Brownian parameter |
| θ | Dimensionless temperature |
| η | Dimensionless similarity variable |
| P | Particle |

## References


[1] M. M. Rashidi, B. Rostami, N. Freidoonimehr and S. Abbasbandy, "Free convective heat and mass transfer for magneto hydrodynamics fluid flow over a permeable vertical stretching sheet in the presence of the radiation and buoyancy effects,". Ain Shams Eng. J., vol.5, no. 3, pp.901-912, 2014,doi: 10.1016/j.asej.2014.02.007.

[2] F. M Hady, F. S. Ibrahim, S. M. Abdel-Gaied and M. R. Eid, "Radiation effect on viscous flow of a nanofluid and heat transfer over a nonlinearly stretching sheet," Nanoscale Res. Lett., vol 7, pp.1-13, 2012,doi: 10.1186/1556-276X-7-229.

[3] F. Aman, A. Ishak, and I. Pop, "Magnetohydrodynamic stagnation-point flow towards a stretching/shrinking sheet with slip effects," Int. Commun. Heat Mass Transf.,vol.47, pp.68-72, 2014,doi: 10.1016/j.asej.2014.02.007.

[4] M. J. Uddin, O. A. Bég, and N. Amin, "Hydromagnetic transport phenomena from a stretching or shrinking nonlinear nanomaterial sheet with Navier slip and convective heating: a model for bio-nano-materials processing," Journal of Magnetism and Magnetic Materials,vol.368,pp.252-261,2014,-doi:10.1016/j.jmmm.2014.05.041.

[5] O. D. Makinde, and A. Aziz, "Boundary layer flow of a nanofluid past a stretching sheet with a convective boundary condition," Int. J. Therm. Sci., vol. 50, pp.1326-1332, 2011, doi:10.1016/j.ijthermalsci.2011.02.019.

[6] Hamad, M. A. A., Kasseb L. Mahny, and M. R. Abdel-Salam. "Similarity solution of viscous flow and heat transfer of nanofluid over a nonlinearly stretching sheet." Middle-East Journal of Scientific Research, vol.8(4) pp. 764-768,2011.

[7] D. Ramya, R. S. Raju, J. A. Rao, and A. J. Chamkha. "Effects of velocity and thermal wall slip on magnetohydrodynamics boundary layer viscous flow and heat transfer of a nanofluid over a non-linearly-stretching sheet: a numerical study," Propuls. Power Res., vol. 7(2),pp.182-195,2018,doi:10.1016/j.jppr.2018.04.003.

[8] B.Ghazi ,S. Kadri , R.Mehdaoui, "Temperature evolution within a solar panel using a cooling source of varying sizes and shapes in the presence of a hybrid nanofluid. "J The Eng vol.11(4),pp-1011–1023,2025.

[9] B. S. Goud, P. Srilatha, D. Mahendar,T. Srinivasulu, and Y.D. Reddy. "Thermal radiation effect on thermostatically stratified magneto hydrodynamics fluid flow through an accelerated vertical porous plate with viscous dissipation impact,"Partial Differ. Equ. Appl. Math.,vol.7,pp.100488,2023,doi:10.1016/j.padiff.2023.100488.

[10] A. B. Jafar., S.Shafie and I. Ullah, "Magneto hydrodynamics radiative nanofluid flow induced by a nonlinear stretching sheet in a porous medium," Heliyon, vol. 6, Issue 6, 2020, e04201, doi:10.1016/j.heliyon.2020.e04201.

[11] B. Ahmad, M. O. Ahmad, M. Farman, A. Akgül, and M.B. Riaz. "A significance of multi slip condition for inclined magneto hydrodynamics nano-fluid flow with non-linear thermal radiations, Dufour and Soret, and chemically reactive bio-convection effect," S. Afr. J. Chem. Eng., vol.43, pp.135-145,2023,doi:10.1016/j.sajce.2022.10.009.

[12] Z.Abbas, I.Mehdi, J. Hasnain, A. K. Alzahrani, and M.Asma,"Homogeneous-heterogeneous reactions in magneto hydrodynamics mixed convection fluid flow between concentric cylinders with heat generation and heat absorption," Case Stud. Therm. Eng., vol. 42,102718, 2023,doi:10.1016/j.csite.2023.102718.

[13] S. R. R. Reddy and P. B.A.Reddy," Thermal radiation effect on unsteady three-dimensional MHD flow of micropolar fluid over a horizontal Surface of a parabola of revolution,"Propuls.Power Res.,vol.11,pp.129-142,2022,doi:10.1016/j.jppr.2022.01.001.

[14] V. R. R Janke, S. Naramgari, and S. Vangala, "Magneto hydrodynamics flow of a nanofluid embedded with dust particles due to cone with volume fraction of dust and nano particles," Procedia Eng.,vol. 127,pp.1026-1033,2015, doi:10.1016/j.proeng.2015.11.452.

[15] M. R. Khan, S. Mao, W. Deebani, and A.M. Elsiddieg,"Numerical analysis of heat transfer and friction drag relating to the effect of Joule heating, viscous dissipation and heat generation/absorption in aligned magneto hydrodynamics slip flow of a nanofluid," Int. Commun. Heat Mass Transf.,vol.131,pp.105843,2022,doi:10.1016/j.cheatmasstransfer.2021.105843.

[16] V.Makkar and P.Batra, "Numerical simulation of magneto hydrodynamics convective nanofluid flow with buoyancy forces over three-dimensional exponential stretching surface," Mater. Today: Proc.,vol 52, pp.810-817,2022,doi: 10.1016/j.matpr.2021.10.169.

[17] R.Geetha , B.Reddappa ,A. Sumithra ,B. R. Kumar , B.P. Reddy. Heat and mass transfer analysis of unsteady MHD Carreu Nanofluid flow over a stretched surface in a porous medium with Stefan blowing condition. J Ther Eng ,vol.11(3),pp.765–779,2025.

[18] S.K.Parida, S.Panda, and B.R.Rout, "Magneto hydrodynamics boundary layer slip flow and radiative nonlinear heat transfer over a flat plate with variable fluid properties and thermophoresis,"Alex. Eng. J.,vol 54, pp.941-953, 2015,doi: 10.1016/j.aej.2015.08.007.

[19] N.S.Anuar, N. Bachok, and I. Pop, "Influence of magneto hydrodynamics hybrid Ferro fluid flow on exponentially stretching/shrinking surface with heat source/sink under stagnation point region," Mathematics ,Nov.2021, vol.9 ,no.22, 2932, doi:10.3390/math9222 932.

[20] S.Sadighi,H.afsher,M.Jabbari,H.A.D Ashtiani,"Heat and Mass transfer for magneto hydrodynamics nanofluid flow on a porous stretching sheet with prescribed boundary conditions." Case studies in thermal Engineering.,vol-49 ,pp.103345, 2023.

[21] B.C.Prasannakumara B. J.Gireesha , M.R.Krishnamurthy .K. Ganesh Kumar, ." MHD flow and nonlinear radiative heat transfer of Sisko nanofluid over a nonlinear stretching sheet." Informatics in Medicine Unlocked.vol.9:pp.123-132, 2017.

[22] I. Tlili, R. Moradi, and M. Barzegar Gerdroodbary. "Transient nanofluid squeezing cooling process using aluminium oxide nanoparticle ,"International Journal of Modern Physics, vol.30(11), pp.1950078 ,2019.

[23] M. B. Gerdroodbary, "Application on neural network on heat transfer enhancement of MHD nanofluid, "Heat transfer Asian research, vol.49(1),pp.197-212,2019.

[24] [24]T.D.Manh,A.M.Abazari,M.B.Gerdroodbary,,N.D.Nam,R. Moradi,H.Babazdeh,"Computational simulation of variable magnetic force on heat characteristics of backward-facing step flow,"Journal of Thermal Analysis and Calorimetry. vol.144, pp.1585–1596, 2020.

[25] T.D.Manh,M.Bahramkhoo,M.B.Gerdroodbary,"Investigation of nanomaterial flow through non-parallel plates," Journal of Thermal Analysis and Calorimetry, vol.143,pp. 3867–3875 ,2021. https://doi.org/10.1007/s10973-020-09352-0.

[26] A.M.Sedki," Effect of thermal radiation and chemical reaction on MHD mixed convective heat and mass transfer in nanofluid flow due to nonlinear stretching surface through porous medium, "Results in Materials, vo1. 6,pp.100334, 2022.

[27] P.P.Humanee,V.S. Patil,A. B. Patil," Effects of radiation and chemical reaction on MHD Casson nanofluid flow past a porous stretching," Computational Thermal Sciences: An International Journal, vol.15(5), pp. 1-15,2023.

[28] M. B. Gerdroodbary, M. Jafaryar, M. Sheikholeslami,Y. Amini, "The efficacy of magnetic force on thermal performance of Ferro fluid in a screw tube,"Case studies in thermal engineering, vol.49,pp.103187,2023.

[29] D. Reddy, I. Mangaonna," Significance of radiation and chemical reaction MHD heat transfer nano fluid flow over a non-linearly porous stretching sheet with non-uniform heat source, "Numerical Heat Transfer Part A: Applications, vol.85(18),pp. 2940-2966,2024.

[30] M.U.Krishna,A.G.V.Kumar, "Chemical reaction, slip effects and non-linear thermal radiation on unsteady MHD Jeffreys nanofluid flow over a stretching sheet, "Case studies in thermal engineering, vol.55,pp.104129,2024.

[31] W. Abbas, A. M. Megahed, E. Fares, "The impact of a chemical reaction on the heat and mass transfer mechanisms in a dissipative and radiative nanofluid flow over a nonlinear stretching sheet," Scientific Reports, vol.14(1),pp.7712,2024.